DESIGN OF LAMINAR SUPERCRITICAL AIRFOILS BASED ON NAVIER-STOKES EQUATIONS

Zhong-Hua HAN, Jie DENG, Jun LIU, Ke-Shi, ZHANG, Wen-Ping SONG
National Key Laboratory of Aerodynamic Design and Research, School of Aeronautics, Northwestern Polytechnical University, Xi'an, 710072, China
hanzh@nwpu.edu.cn;
djcameron@163.com;13474476499@139.com;wpsong@nwpu.edu.cn;zhangkeshi@nwpu.edu.cn

Keywords: *laminar airfoil; supercritical airfoil; aerodynamic optimization; surrogate model*

Abstract

This paper aims to develop a suit of design methods and tools for laminar supercritical airfoils, based on high-fidelity computational fluid dynamics (CFD). The reliable transition perdition method, efficient inverse design and global optimization design methods are regarded as three key issues, which are addressed in this paper. The automatic transition prediction method coupling Navier-Stokes equations flow solver and e^N linear stability analysis method is applied to the design and analysis of the laminar supercritical airfoils; inverse design and optimization design methods based on kriging surrogate model is developed to attain favorable pressure gradient while reducing wave drag; efficient optimization based on kriging model and an improved EI (expected improvement) method is developed for finding the global optimum. Two laminar supercritical airfoils have been designed for cruise Mach number of 0.72 and 0.74, and design lift coefficient of 0.6. The results show that about 55-60 laminar flow regions on upper- and lower surface have been attained.

1 Introduction

Due to the severe environmental impact of growing air travel, reducing fuel consumption and CO_2 emissions has become an important long-term goal in aerospace community [1]. For example, the Advisory Council for Aeronautics Research in Europe (ACARE) has set a goal that the fuel consumption and CO_2 emissions of transport aircraft should be reduced by 50% until 2020 relative to the consumption in 2000. From an aerodynamic point of view, it means that the aerodynamic drag should be remarkably reduced (at least by 15% - 20% [2]). For the aerodynamic design of modern transport aircraft, this is very demanding since the aerodynamic configuration (such as A350 or Boeing 787) has been highly optimized. Therefore, revisiting laminar flow technology has gained high priority for the research and development of drag-reduction technologies that may be applied to future transport aircraft. Among the key aspects associated with attaining laminar flow over a supercritical wing of a transport aircraft, the design of laminar airfoils at transonic regime is particularly challenging and thus of particular importance.

For design of a laminar supercritical airfoil, the main challenge lies on how to attain sufficient favorable pressure gradient over forward part of the airfoil, at the presence of supersonic flow region and without paying the price of wave drag. To address this challenge, reliable method for accurately predicting the aerodynamic prediction considering the flow transition, efficient inverse design and global optimization design methods based on high-fidelity CFD are regarded as three key issues.

Over the past three decades, aerodynamic design via Computational Fluid Dynamics (CFD) has received increasing attentions from the researchers in the aerodynamic community. The focus of CFD applications has shifted to aerodynamic design, since CFD has matured to an extent that high-fidelity CFD, such as Navier-Stokes (NS) is routinely applied to very complex configurations or complicated

aerodynamics design problems. While the performance of computing is growing rapidly in the modern world, the demand for more accurate computer simulation is also growing. Hence, it is still rarely feasible to search a design space directly using expensive computer codes such as high fidelity CFD and CSD codes. The use of surrogate models, then, is of great interest and playing an increasingly important role in the aerodynamic and multidisciplinary design optimization [3][4][5].

This paper aims to develop a suit of efficient design methods and tools for design of laminar supercritical airfoils based high-fidelity CFD. The design exercise of two laminar supercritical airfoils preliminarily shows that they are successfully applied to laminar supercritical airfoil design.

1 Numerical Simulation Methods

An in-house CFD code called PMNS2D [6][7] is used to simulate of the flows around airfoils. A transition prediction module based on e^N method is available for prediction the impressible and compressible flow transition. Besides the in-house CFD code, MSES code [8] developed by Prof. Drela is also used to validate the results. The RANS solver with transition perdition is described blow.

1.1 RANS solver

An integral form of the preconditioned 2-D compressible RANS equations can be written as

$$\iiint_{\Omega} \mathbf{P}\frac{\partial \mathbf{W}}{\partial t}dV + \iint_{\partial\Omega} \overline{\overline{\mathbf{H}}} \bullet \mathbf{n}dS = \iint_{\partial\Omega} \overline{\overline{\mathbf{H}_v}} \bullet \mathbf{n}dS\,, \qquad (1)$$

where $\mathbf{W} = (\rho, \rho u, \rho v, \rho e)^{\mathrm{T}}$ denote the conservative variables; $\mathbf{P}$ is the preconditioning matrix; $\overline{\overline{\mathbf{H}}}$ and $\overline{\overline{\mathbf{H}_v}}$ denote the inviscid and viscous flux vectors, respectively. Note that the influence of preconditioning matrix $\mathbf{P}$ can be removed when the steady solution is achieved. By using such a preconditioning method, the convergence as well as accuracy of flow solver for low-speed flow can be dramatically improved.

For the CFD code, the control equations are solved by a cell-centered finite-volume scheme. A central scheme proposed by Jameson et al is utilized for spatial discretization, and LU-SGS scheme is implemented for time integration. The turbulence viscous coefficient is calculated by Spalart-Allmaras one-equation turbulence model. To improve the efficiency and robustness of the compressible CFD code for low-speed flows or flows with low-speed flow region, a preconditioning method proposed by Turkel [9]. It is implemented within the framework of a Full Approximation Storage (FAS) multigrid method. The detailed description about the numerical scheme can be found in [1] and [7].

1.2 Transition Prediction Based on e^N Method

Unlike the simplified e^N method, such as the e^N-database method [10][11], which detects the transition location with the aid of transition data-base and therefore is not flexible, the present full e^N method based on the spatial amplification is convenient at the cost of solving the compressible linear stability equation for two-dimensional flows. After the velocity and temperature profiles are obtained, the two dimensional linear stability equations are solved by the Newtonian method and Block-Elimination method. The precise initial value for the Newton method is supplied by the continuing method [12].

The RANS solver with transition prediction is shown in Figure 1.

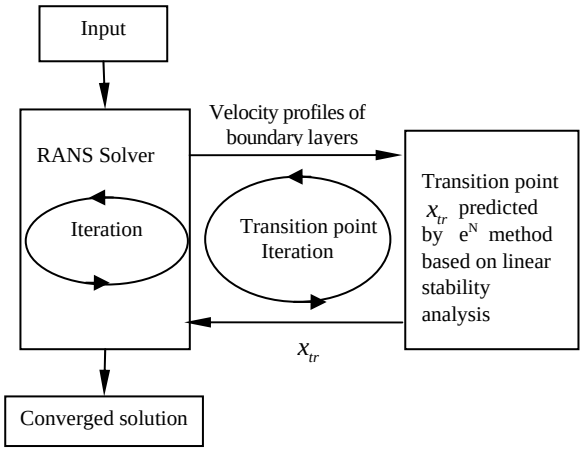

Figure 1 Flowchart of the RANS Solver with the functionality of automatic transition prediction.

2 Overview of Kriging

Kriging is a statistical interpolation method suggested by Krige [13] in 1951 and mathematically formulated by Matheron [14] in 1963. Kriging was widely used in the context of geostatistical problems. In 1989, kriging was extended by Sacks et al [15] for the design and analysis of deterministic computer experiments. See [16][17] for the further extension of kriging model to variable-fidelity surrogate modeling problems via cokriging or gradient-enhanced kriging.

2.1 Kriging Predictor and Mean Squared Error

For an *m*-dimensional problem, suppose we are concerned with the prediction of the output of a high-fidelity, thus expensive computer code, which is correspondent to an unknown function $y:\mathbb{R}^m \to \mathbb{R}$. By running the computer code, y is observed at n sites (determined by DoE)

$$\mathbf{S} = [\mathbf{x}^{(1)},...,\mathbf{x}^{(n)}]^T \in \mathbb{R}^{n\times m}, \mathbf{x} = \{x_1,..,x_m\} \in \mathbb{R}^m \qquad (2)$$

with the corresponding responses

$$\mathbf{y}_S = [y^{(1)},...,y^{(n)}]^T = [y(\mathbf{x}^{(1)}),...,y(\mathbf{x}^{(n)})]^T \in \mathbb{R}^n . \qquad (3)$$

The pair $(\mathbf{S}, \mathbf{y}_S)$ denotes the sampled data sets in the vector space.

With the above descriptions and assumptions, our objective here is to build a surrogate model for predicting the output of the computer code for any untried site $\mathbf{x}$ (that is, to estimate $y(\mathbf{x})$) based on the sampled date sets $(\mathbf{S}, \mathbf{y}_S)$, in an attempt to achieve the desired accuracy with the least possible number of sample points.

The kriging treats the output of a deterministic computer experiment as a constant term plus a stochastic process:

$$Y(\mathbf{x}) = \beta + Z(\mathbf{x}) . \qquad (4)$$

The stationary random process $Z(\bullet)$ has mean zero and covariance of

$$Cov[Z(\mathbf{x}), Z(\mathbf{x}')] = \sigma^2 R(\mathbf{x},\mathbf{x}') , \qquad (5)$$

where σ^2 is the process variance of $Z(\bullet)$ (it is assumed that $\sigma^2(\mathbf{x}) \equiv \sigma^2$ for all $\mathbf{x}$, and R is the spatial correlation function that only depends on the Euclidean distance between two sites $\mathbf{x}$ and $\mathbf{x}'$.

With above assumptions, the kriging predictor can be derived, which is of the form (see [5][15][16][17] for detailed derivation)

$$\hat{y}(\mathbf{x}) = \beta_0 + \mathbf{r}^T(\mathbf{x})\mathbf{R}^{-1}(\mathbf{y}_s - \mathbf{1}\beta_0) , \qquad (6)$$

where $\mathbf{1}$ is unit column vector filled with ones and

$$\beta_0 = \left(\mathbf{1}^T\mathbf{R}^{-1}\mathbf{1}\right)^{-1}\mathbf{1}\mathbf{R}^{-1}\mathbf{y}_S , \qquad (7)$$

and

$$\mathbf{R} := \left[R(\mathbf{x}^{(i)}, \mathbf{x}^{(j)})\right]_{ij} \in \mathbb{R}^{n\times n}, \mathbf{r}(\mathbf{x}) := \left[R(\mathbf{x}^{(i)}, \mathbf{x})\right]_i \in \mathbb{R}^n . \qquad (8)$$

The MSE of the kriging prediction at any untried $\mathbf{x}$ can be proven to be

$$MSE[\hat{y}(\mathbf{x})] = \hat{s}^2 = \hat{\sigma}^2[1 - \mathbf{r}^T\mathbf{R}^{-1}\mathbf{r} + (1 - \mathbf{1}\mathbf{R}^{-1}\mathbf{r})^2 / \mathbf{1}^T\mathbf{R}\mathbf{1}] , \qquad (9)$$

where

$$\hat{\sigma}^2 = \frac{1}{n}(\mathbf{y}_s - \mathbf{1}\beta_0)^T\mathbf{R}^{-1}(\mathbf{y}_s - \mathbf{1}\beta_0). \qquad (10)$$

2.2 Correlation Models

The construction of the correlation matrix $\mathbf{R}$ and the correlation vector $\mathbf{r}$ requires the calculation of the correlation functions. The correlation function for random variables at two sites $\mathbf{x}^{(i)}, \mathbf{x}^{(j)}$ is assumed to be only dependent on the spatial distance. Here we focus on a family of correlation models that are of the form

$$R(\mathbf{x}^{(i)}, \mathbf{x}^{(j)}) = \prod_{k=1}^{m} R_k(\theta_k, \mathbf{x}_k^{(i)} - \mathbf{x}_k^{(j)}) . \qquad (11)$$

The correlation function used here is the cubic spline:

$$R_k = \begin{cases} 1 - 15\xi_k^2 + 30\xi_k^3 & \text{for } 0 \le \xi_k \le 0.2 \\ 1.25(1-\xi_k)^3 & \text{for } 0.2 < \xi_k < 1 \\ 0 & \text{for } \xi_k \ge 1 \end{cases} , \qquad (12)$$

where

$$\xi_k = \theta_k \left|\mathbf{x}_k^{(i)} - \mathbf{x}_k^{(j)}\right|. \qquad (13)$$

2.3 Kriging Fit

Hyper parameters of kriging, $\boldsymbol{\theta} = (\theta_1, ..., \theta_m)$, can be tuned by solving maximum likelihood estimation (MLE) problem:

$$\text{MLE} = \arg\max_{\boldsymbol{\theta}} \left(-\frac{1}{2} \left[n_s \ln(\hat{\sigma}^2) + \ln |\mathbf{R}| \right] \right) . \quad (14)$$

In this paper, the quasi-Newton method is used for such a sub-optimization problem.

3 Use of Kriging Surrogate Model for Optimization

After the surrogate model is constructed, the global optimum may not be found, since the model is not accurate. Additional points should be infilled both to increase the accuracy of the model and to explore the design space. In this paper, multiple infill strategies can be switched or implemented simultaneously (also see [5] [20][21] for detailed description).

3.1 Constrained Expected Improvement (EI_c)

Expected improvement is defined as the improvement we expect to achieve at an untried site $\mathbf{x}$. Assume the random variable $Y \sim N[\hat{y}(\mathbf{x}), s^2(\mathbf{x})]$, where $\hat{y}$ is the kriging predictor， s^2 is mean square error defined in Eq. Let $y_{\min}$ is the current best objective function value; the improvement is $I = y_{\min} - Y(\mathbf{x}) > 0$. The expected improvement [18][19] is given by

$$E[I(\mathbf{x})] = \begin{cases} (y_{\min} - \hat{y}(\mathbf{x}))\Phi\left(\frac{y_{\min} - \hat{y}(\mathbf{x})}{s(\mathbf{x})}\right) + s \times \phi\left(\frac{y_{\min} - \hat{y}(\mathbf{x})}{s(\mathbf{x})}\right) & \text{if } s>0 \\ 0 & \text{if } s=0 \end{cases} , \quad (15)$$

where $\Phi(\bullet)$ and $\phi(\bullet)$ are the cumulative distribution function and probability density function of standard normal distribution, respectively.

Assume we have a constraint $g(\mathbf{x}) > g_{\min}$, and we also constructed a kriging model for $g(\mathbf{x})$. Following the same logic of the expected improvement, we assume the random variable $G \sim N[\hat{g}(\mathbf{x}), s^2(\mathbf{x})]$. Then, the probability that the constraint is fulfilled is as following:

$$P[G > g_{\min}] = \Phi\left(\frac{g_{\min} - \hat{g}(\mathbf{x})}{s(\mathbf{x})}\right), \quad (16)$$

where s is the variance of the kriging model of the constraint. Then, the constrained expected improvement is:

$$E_c[I(\mathbf{x})] = E[I(x) \cap G > g_{\min}] = E[I(\mathbf{x})] \bullet P[G > g_{\min}] . \quad (17)$$

For multiple constraints, the constrained expected improvement is obtained by multiplying each probability that the constraints fulfilled.

The greater the EI_c, the more improvement we expect to achieve, thus the point with maximum EI_c is found then observed and infilled to the sample set to refine the kriging model. This criterion is considered a type of "balanced exploration and exploitation"[4].

3.2 Minimizing the Predictor (MP)

This criterion assumes that the surrogate model is globally accurate and we only need to validate the optimum of the surrogate. The optimum point on the surrogate is found and observed to refine the kriging model. It is considered a type of "exploitation"[4]. In this paper, the minimization problem is solved by genetic algorithm (GA), and the constraints are handled by the GA itself. Here, real coded GA is implemented. Following Kalyanmoy [22], simulated binary crossover and parameter-based mutation operator is utilized; and the constraints are handled as follows: first all constraints are transformed to the form $g >= 0$ and normalized. The fitness function is defined as

$$F(\mathbf{x}) = \begin{cases} y(\mathbf{x}) & \text{if } g_j(\mathbf{x}) \geq 0 \ \ \forall j=1,2,...,m \\ y_{\max} + \sum_{j=1}^{n_c} \langle g_j(\mathbf{x}) \rangle & \text{otherwise} \end{cases} , \quad (18)$$

where n_c is the number of the constraints, and $\langle\ \rangle$ denotes the absolute value of the operand if the operand is negative, and returns a value zero otherwise. The parameter $y_{\max}$ is the objective function value of the worst feasible solution in the population.

3.3 Framework of the Kriging-Based Optimization Method

In this research, a kriging-based optimization system is used [21]. First, several initial sample points are generated in the design space using design of experiments (DoE). Here, we use the Latin hypercube sampling (LHS) [23]; then the samples are observed with parallel computing to save total clock time; after that, the kriging models are constructed both for objective function and constraints, then the kriging models are refined repetitively by infilling new points obtained with GA under specified infill criteria; this iteration terminates until some stop criteria meet, for instance, the function evaluation budgets exceeds some specified value. The framework of the optimization is shown in Figure 2

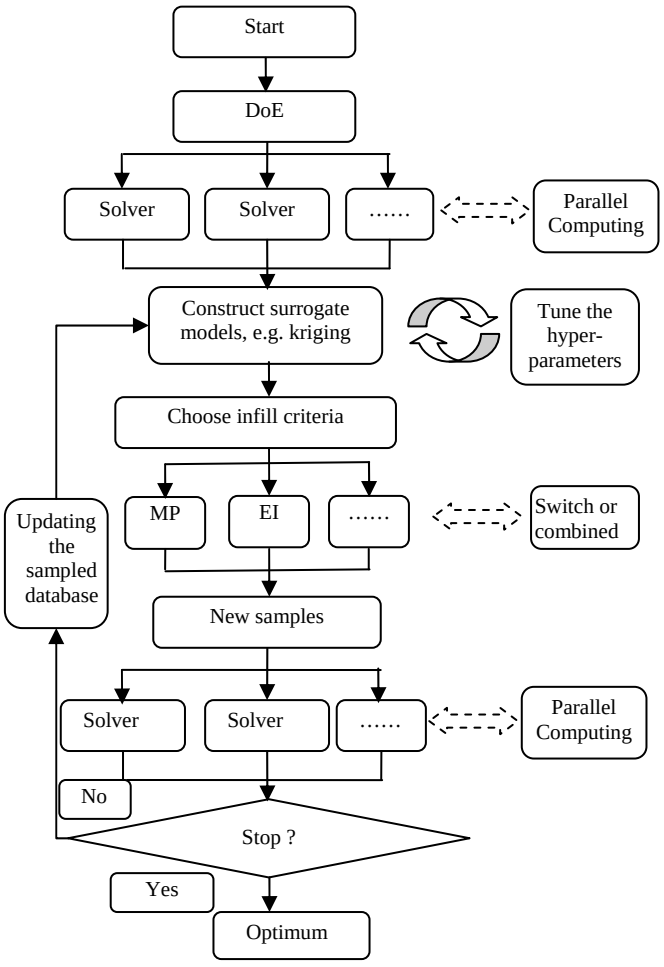

Figure 2 Framework of the kriging-based optimization method

4 Results

4.1 Validation of the Surrogate-based Optimizer for Airfoil Drag Minimization

First example is the drag minimization of an RAE 2822 airfoil (see Figure 3 for the computational grid), which is a benchmark for testing the optimizer. The iterative response-surface model (RSM)-based optimizer is implemented to be compared with the kriging-based optimizer. These two optimizers are compared for the drag minimization of an RAE2822 airfoil. The mathematical model is as following

$$\begin{aligned} \textit{Objective} &: \text{Minimize} \quad c_d \\ \textit{s.t.} &: (1)\ c_l \geq c_{l0} \\ &: (2)\ |c_m| \leq |c_{m0}| \\ &: (3)\ \textit{Thickness} \geq \textit{Thickness}_0 \end{aligned}, \tag{19}$$

where $\textit{Thickness}_0$ denotes the maximum thickness of the baseline airfoil. 10 Hicks-Henne bump functions [24] are used to deform the airfoil, with 5 on the lower and upper surfaces, respectively; the amplitude of the functions are designated as design variables, hence, we have 10 design variables in total.

For the kriging-based optimizer, 20 initial sample points are generated by LHS. EI as well as MP infill criteria are used simultaneously, thus two points are infilled to refine the surrogate models at each iteration.

For the RSM-based optimizer, we used the second-order polynomials to construct the response surfaces. There are $n = (m+2)(m+1)/2$ coefficients for m variables. To obtain a reasonably accurate response surface, 1.5m sample points are needed for relatively small problems (5-10 variables). Hence, 99 initial sample points are generated by LHS in this example. Similar to the kriging-based optimizer, once the response surface is constructed, the constrained optimization problem is solved using genetic algorithm. The response surfaces are refined repetitively by infilling the newly sampled data. This iteration is terminated until the evaluation budget exceeds 15 times of the dimensionality.

Table 1 shows the optimization results of the two optimization methods. The two optimized and baseline airfoils and the corresponding pressure coefficient distributions are compared

in. Figure 5 shows the convergence history of the two optimizers. Obviously, the kriging-based optimization method gives higher drag reduction percentage with much higher efficiency. This confirms the superiority of kriging over the RSM, and demonstrates that the kriging-based optimizer is more likely to find the global optimum.

Table 1 Optimization results of RAE2822 airfoil

	c_d	c_l	$\lvert c_m \rvert$	Thickness	Runs of flow solver
Baseline	100	100	100	100	-
Kriging	72.4 (-27.6%)	100.6 (+0.6%)	94.0 (-6.0%)	100.0 (+0.0%)	52
RSM	75.1 (-24.9%)	101.9 (+1.9%)	92.9 (-7.1%)	100.0 (+0.0%)	150

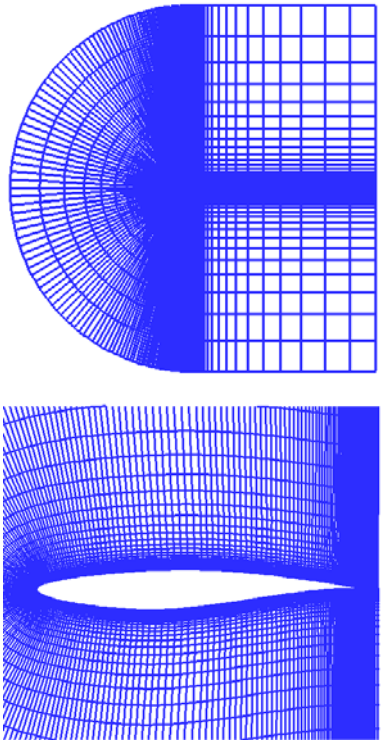

Figure 3 Computational grid for RAE 2822 airfoil

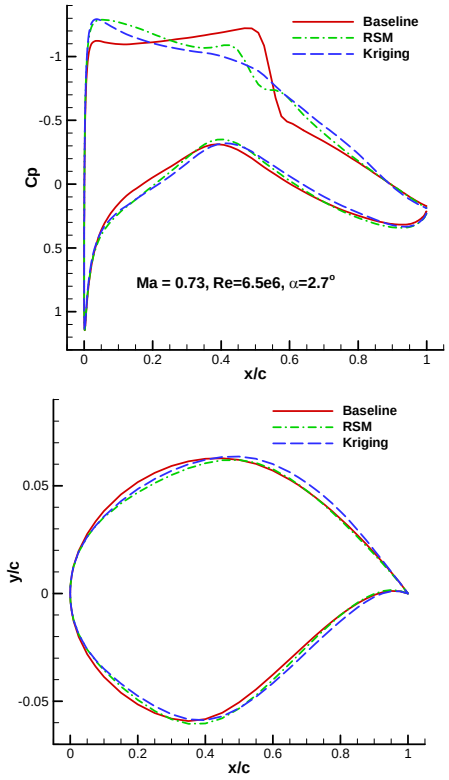

Figure 4 Comparison of pressure coefficient distributions and geometries of optimized and baseline airfoils.

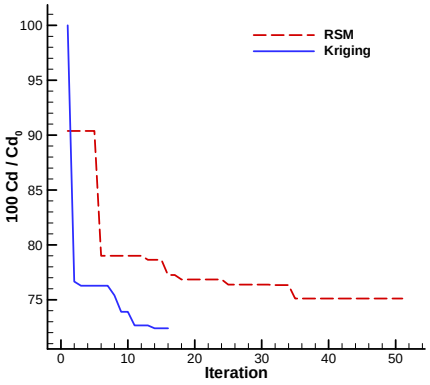

Figure 5 Convergence history of the kriging- and RSM-based optimizers

4.2 Validation of the Surrogate-Based Optimizer for Airfoil Inverse Design

A kriging-based single- and multi-point inverse design method is developed and investigated. Compared with the drag minimization of an airfoil based on kriging models, the MP sampling refinement criterion is used instead of EI, since the inverse design is a local optimization problem. The objective function of the inverse design problem is:

$$J = \sum_{B_w} \left(C_p - C_{p0} \right)^2 , \qquad (20)$$

where C_p is the pressure coefficient of the current airfoil, and C_{p0} is the pressure coefficient of the target airfoil; B_w is the wall boundary.

Kulfan's CST [25] method is used to represent the airfoils instead of the Hicks-Henne bump functions. Unlike gradient-based inverse design methods, the design space should be designated instead of an initial airfoil. We first prescribe a "thick" shape and a "thin" shape, and then the two shapes are fitted by CST. We treat the CST parameters of the "thin" shape as the lower bound of the design variables, while the parameters of the "thick" shape as the upper bound. For real engineering problems, the geometry of the target airfoil is unknown, hence, one have to first prescribe the "thick" and "thin" shapes that covering the unknown target airfoil. As an example, the design space of the inverse designs in this paper is obtained by the 2 shapes shown in Figure 6, and 19 design variables were used.

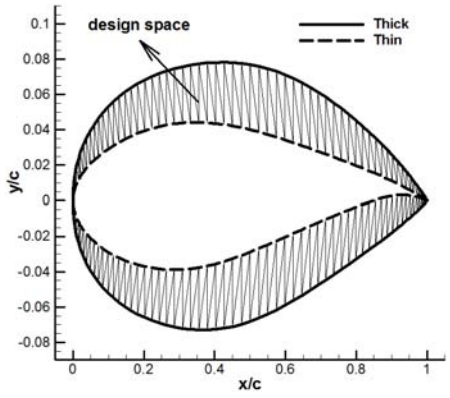

Figure 6 Definition of design space for inverse design

Our target is to obtain the REA2822 airfoil when given its pressure coefficient distribution on the airfoil boundary at the flow condition of $Ma = 0.73$, α=2°, $\mathrm{Re} = 6.5 \times 10^6$.

Figure 7 shows the comparison of pressure coefficient distributions and geometries of the target airfoil and designed airfoil. We see that both the geometry of the designed airfoil and its pressure coefficient coincide well with the target airfoil's. Figure 8 shows the convergence history of the objective function; note that the square symbols ahead of the vertical line denote the initial sample points.

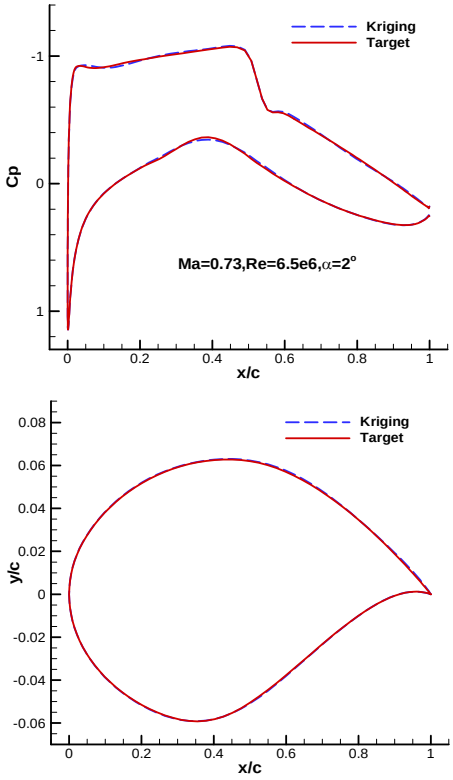

Figure 7 Comparison of the pressure coefficient distributions and the geometries for an inverse design

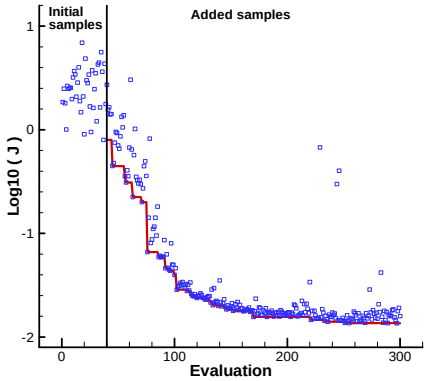

Figure 8 Convergence history of the objective function for single point inverse design

4.3 Design Results for Laminar Supercritical Airfoils

Two airfoils, named LSC 72613 and LSC 74611, have been design, using the combination of inverse design, optimization design and directly modification of the geometry. The design states of these two airfoils are:

$$\begin{aligned} &LSC72613: Ma = 0.72, \mathrm{Re} = 2.0E7, C_l = 0.6 \\ &LSC74611: Ma = 0.74, \mathrm{Re} = 2.0E7, C_l = 0.6 \end{aligned} \qquad (21)$$

The aerodynamic properties of designed airfoils at full turbulent and free transition conditions

are investigated. The aerodynamic properties off the design state are also studied. The aerodynamics properties are shown in Table 2, Figure 9 and Figure 10. About 55 – 60% laminar flows are attained at the both side of the airfoils, which yields higher lift-to-drag than conventional supercritical airfoils.

Table 2 Aerodynamic performance of LSC 72613 and LSC 74611 airfoils (free transition)

Airfoils	Thickness	Lift	Drag	Moment	L/D
LSC 72613	12.9%c	0.60	0.0046	-0.137	130
LSC 74611	11.3%c	0.60	0.0049	-0.134	122

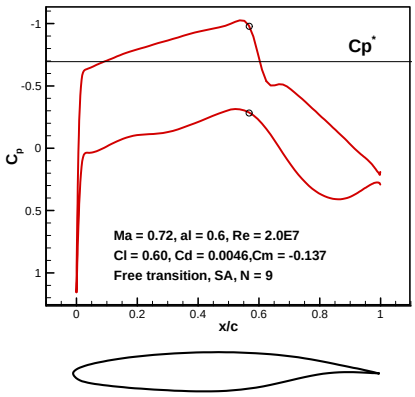

a) Free transition Cp

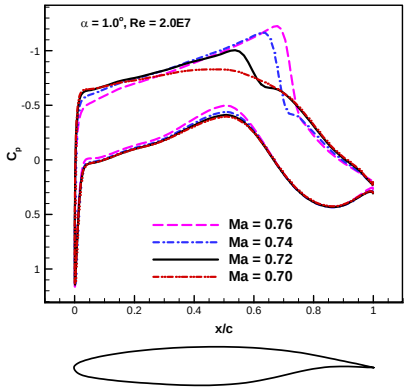

b) Full turbulence Cp

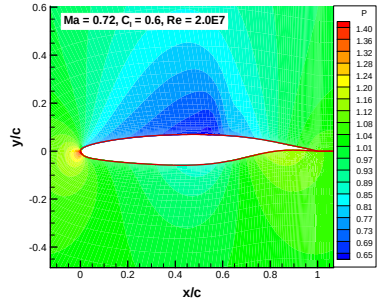

c) Pressure contour

Figure 9 Aerodynamic properties of LSC 72613 airfoil

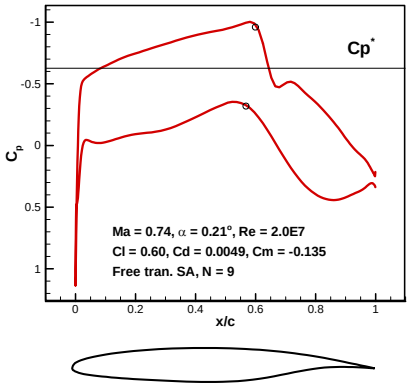

a) Free transition Cp

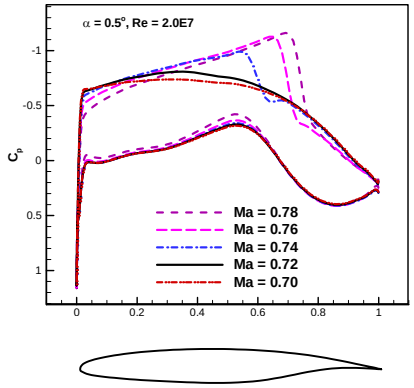

b) Full turbulence Cp

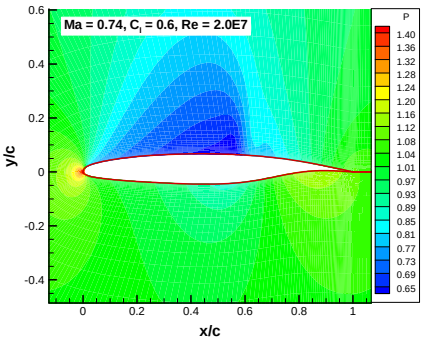

c) Pressure contour

Figure 10 Aerodynamic properties of LSC 74611 airfoil

5 Conclusions and Discussion

A suite of design methods and tools have been developed to address the challenge of designing laminar supercritical airfoils. Design excise of two laminar supercritical airfoils, LSC 72613 and LSC 64611, preliminarily shows that the development of the design methods and tools are successful.

The wind tunnel test will be conducted for these two airfoils to further validate the design methods. Extension of the methods and tools to laminar supercritical wind design are subjects of future work.

Acknowledgements

This research was sponsored by the National Natural Science Foundation of China (NSFC) under grant No. 10902088, the Aeronautical Science Foundation under grant No. 2011ZA53008 and the National Technology Research and Development Program of China under grant No. 2012AA051301.

References

[1] Green, J. E., "Laminar Flow Control – Back to the Future?" AIAA paper 2008-3738, 2008.

[2] Horstmann, K. H., Streit, T., "Aerodynamic Wing Design for Transport Aircraft – Today", R. Radespiel et al. (Eds.): Hermann Schlichting – 100 Years, Springer, NNFM 102, 2009, pp. 130–144.

[3] Queipo, N. V., Haftka, R. T., Shyy, W., Goel, T., Vaidyanathan, R., and Tucher, P. K., "Surrogate-based Analysis and Optimization," *Progress in Aerospace Sciences*, Vol. 41, 2005, pp. 1-28.

[4] Forrester, A. I. J., and Keane, A. J., "Recent advances in surrogate-based optimization," *Progress in Aerospace Sciences*, Vol. 45, No. 1–3, Jan.–April 2009, pp. 50–79.doi:10.1016/j.paerosci.2008.11.001

[5] Han, Z. -H., Zhang, K. -S, "Surrogate Based Optimization," Intec Book, *Real-world Application of Genetic Algorithm*, 2012, pp.343-362.

[6] Xie, F. -T., Song, W. -P., and Han, Z. -H., "Numerical Study of High-Resolution Scheme Based on Preconditioning Method," *Journal of Aircraft*, Vol. 46, No. 2, 2009, pp. 520-525.

[7] Han, Z. -H., He F., Song, W. -P., and Qiao, Z. -D., "A preconditioned multigrid method for efficient simulation of three-dimensional compressible and incompressible flows", *Chinese Journal of Aeronautics*, Vol. 20, No. 4, 2007, pp. 289-296.

[8] Drela, M., "Newton solution of coupled viscous/inviscid multielement airfoil flows," AIAA 21st Fluid Dyn., Plasma Dyn. and Lasers Conf., AIAA-90-1470, June 1990.

[9] Turkel, E., Radespiel, R., and Vatsa, V. N., "Preconditioning Methods for Low Speed flows," AIAA paper 96-2460, 1996.

[10] Stock, H. W., Degenhardt, E., "A Simplified eN Method for Transition Prediction in Two-dimensional, Incompressible Boundary Layers," Zeitung für Flugwissenschaft und Weltraumforschung 1989, 13: 16-30.

[11] Casalis, G.., Arnal, D., "ELFIN II Subtask 2.3: Database Method – Development and Validation of the Simplified Method for Pure Crossflow Instability at Low Speed," ELFIN II – European Laminar Flow Investigation, Technical Report No. 145, ONERA-CERT, Départment d'e tudes et de Recherches en Aerothermodynamique (DERAT), R.T. DERAT No. 119/5618.16, December 1996.

[12] Cebeci, T., "Stability and Transition: Theory and Application," New York: Springer-Verlag Berlin Heidelberg, 2004.

[13] Krige, D. G., "A Statistical approach to some basic mine valuations problems on the Witwatersrand," *Journal of the Chemical, Metallurgical and Mining Engineering Society of South Africa*, Vol. 52, No. 6, 1951, pp. 119-139.

[14] Matheron, G. M., "Principles of geostatistics. *Economic Geology*," Vol. 58, No. 8, 1963, pp. 1246-1266.

[15] Sacks, J., Welch, W. J., Mitchell, T. J., and Wynn, H. P., "Design and analysis of computer experiments," *Statistical Science*, Vol. 4, 1989, pp. 409-423.

[16] Han, Z. -H., Zimmermann, R., and Görtz, S., "An Alternative Cokriging Model for Variable-Fidelity Surrogate Modeling," *AIAA Journal*, Vol 50, No. 5, 2012, pp.1205-1210. doi: 10.2514/1.J051243 .

[17] Han, Z. -H., Görtz, S., and Zimmermann, R., "Improving Variable-Fidelity Surrogate Modeling via Gradient-Enhanced Kriging and a Generalized Hybrid Bridge Function," *Aerospace Science and Technology* (2012), doi:10.1016/j.ast.2012.01.006.

[18] Jones, D. R., Schonlau, M., and Welch, W. J., "Efficient global optimization of expensive black-box functions," *Journal of Global Optimization*, Vol.13, 1998, pp.455-492.

[19] Jeong, S., Murayama, M., and Yamamoto, K., "Efficient Optimization Design Method Using Kriging Model," *Journal of Aircraft*, Vol. 42, No. 2, 2005, pp. 413- 420.

[20] Song, W. P., Xu, R. F., and Han, Z. H. Study on the improving kriging-based optimization design method. *27th international congress of the aeronautical science s*, Nice, France, 2010.

[21] Liu, J., Han, Z. H., and Song, W. P.. "Efficient kriging-based optimization design of transonic airfoils: some key issues," AIAA Paper 2012-0967, 2012.

[22] Deb, K., "An efficient constraint handling method for genetic algorithms," *Computer Methods in applied Mechanics and Engineering*, Vol. 186, 2000, pp.311-338.

[23] Giunta, A. A., Wojtkiewicz, S. F. J., and Eldred, M. S., "Overview of modern design of experiments methods for computational simulations," AIAA Paper 2003-649, 2003.

[24] Hicks, R. M., and Henne, P. A., "Wing Design by Numerical Optimization," Journal of Aircraft, Vol. 15, No. 7, 1978, pp. 407–412.

[25] Kulfan, B. M., "Universal Parametric Geometry

Representation Method, ”Journal of Aircraft , Vol. 45, No. 1: 2008, pp.142-158

Copyright Statement